The drying tendency of shallow meridional circulations in monsoons

Jun Zhai*, William Boos

Department of Geology and Geophysics, Yale University, New Haven, Connecticut, USA

*Correspondence to: jun.zhai@yale.edu

Shallow meridional overturning circulations are superimposed on the deep circulations that produce precipitation in nearly all monsoon regions, and these shallow circulations transport subtropical, mid-tropospheric dry air into the tropical monsoon precipitation maxima. Here horizontal moisture advection produced by shallow meridional circulations is characterized in the monsoon regions of West Africa, South Asia, Australia, and southern Africa during local summer. Horizontal flow in the upper and lower branches of the shallow meridional circulations consistently dries and moistens air, respectively, in the continental precipitation maxima of each region. The peak drying by horizontal advection occurs at a lower altitude than the peak winds in the upper branch of the shallow circulations. Advection of time-mean moisture by time-mean wind dominates horizontal moisture advection in South Asia and West Africa, while most horizontal moisture advection in Australia and southern Africa is produced by transient eddies. Much of the transient eddy advection can be accurately represented as a first-order horizontal diffusion with a constant, globally uniform diffusivity. These results suggest that horizontal moisture advection in theoretical and conceptual models of seasonal mean monsoons can be adequately represented in terms of time-mean winds plus a simple horizontal moisture diffusion.

Key Words: Shallow meridional circulations; Monsoons; Tropical dynamics; Eddies; Drying tendency

Received . . .

1. Introduction

The full vertical distribution of atmospheric moisture exerts a profound influence on tropical precipitation. Traditionally, near-surface moisture has been most closely associated with the readiness of an atmospheric column to precipitate because the humidity and temperature of air parcels below the lifted condensation level determine the amount of potential energy available for moist convection. More recently, the ability of mid-tropospheric dry air to inhibit precipitation has been appreciated. Precipitation, the depth of convective clouds, and the net upward convective mass flux have all been shown to be highly sensitive to dry air above the base of cumulus clouds, in both observations (e.g. Austin and Fleisher 1948; Sherwood 1999; Yoneyama and Parsons 1999; Holloway and Neelin 2009) and numerical simulations (e.g. Tompkins 2001; Derbyshire *et al.* 2004). Time tendencies of lower- and middle-tropospheric humidity due to non-convective processes — principally surface evaporation and advection by large-scale flow — can thus strongly influence the distribution of tropical precipitation.

The horizontal advection of humidity has been shown to be of particular importance in governing the intensity and structure of monsoon precipitation. Chou *et al.* (2001) showed that advection of cold and dry extratropical air into monsoon regions disfavors monsoon precipitation and limits the poleward expansion of monsoons during local summer. Orography was argued to create a strong South Asian monsoon by suppressing the penetration of dry, low-energy extratropical air into the monsoon thermal maximum (Chakraborty *et al.* 2006; Boos and Kuang 2010); more recent work has emphasized that it is the horizontal advection of hot and dry desert air rather than cold and dry extratropical air that would inhibit South Asian rainfall in the absence of orography (Boos and Hurley 2013; Boos 2015). Most of these studies of horizontal moisture advection in monsoons have focused on near-surface humidity (e.g. Privé and Plumb 2007; Nie *et al.* 2010) or have assumed that the entire vertical distribution of humidity increases with the near-surface humidity (Neelin and Zeng 2000).

Indeed, monsoons are commonly thought of as deep overturning circulations that can be fully described by a first-baroclinic mode structure having convergence in the lower and middle troposphere and divergence in the upper troposphere. Specifically, air ascends in the summer monsoon region, flows across the equator, and subsides in the winter hemisphere (e.g. Peixoto and Oort 1992). However, recent work has shown that shallow circulations also exist in the lower and middle troposphere in nearly all monsoon regions. In these shallow circulations, air ascends in the lower troposphere at least 500 km poleward of the monsoon precipitation maximum, then flows toward the equator in the middle troposphere, typically in the 500-800 hPa layer (Zhang *et al.* 2008; Kawamura *et al.* 2002). The low-level flow that feeds

the time-mean ascent in these shallow meridional circulations (SMCs) is superimposed, in the planetary boundary layer, on the low-level inflow to the deep, precipitating monsoon circulation. An SMC in the tropical East Pacific has some similarities to the SMCs observed in monsoon regions, except that in the East Pacific the ascent branch of the SMC is collocated with the ascent branch of the deep, precipitating circulation (Zhang *et al.* 2004; Nolan *et al.* 2007). In contrast, ascent in monsoon SMCs typically occurs over the deserts that lie poleward of the deep, precipitating ascent (e.g. Nie *et al.* 2010). In an empirical decomposition of global monsoon winds in an atmospheric reanalysis, Trenberth *et al.* (2000) found that the first-baroclinic deep mode accounted for 60% of the seasonal cycle variance of divergent flow, while a shallow mode accounted for 20% of that variance.

These shallow circulations have been argued to influence monsoon precipitation through advection of moisture, with most studies of this effect focusing on the West African monsoon. The lower branch of an SMC in a monsoon region transports relatively cool and moist air poleward across the precipitation maximum, producing near-surface cooling and moistening poleward of that precipitation maximum via horizontal advection. This has been argued to help shift the West African precipitation maximum northward in the early summer phase of its seasonal cycle (Thorncroft *et al.* 2011). At the same time, the upper branch of the SMC transports hot, dry air toward the equator, warming and drying the precipitation maximum in the lower to middle troposphere. The horizontal advective tendencies produced by the West African SMC thus form a vertical dipole, with cooling and moistening in the lowest 1-2 km of the atmosphere over the Sahel and Sahara, and warming and drying above that up to about 5 km (Peyrillé and Lafore 2007). Zhang *et al.* (2008) suggested that the mid-level advective warming and drying prevents the West African precipitation maximum from shifting northward during early summer, allowing a later abrupt northward jump when sufficient convective instability has accumulated (see also Sultan *et al.* 2000; Gu and Adler 2004). Similarly, Xie *et al.* (2010) used field campaign data to show that mid-level drying due to horizontal advection contributed to the limited vertical growth of clouds over northern Australia during suppressed episodes of that region's local summer monsoon. Yet another example was discussed by Parker *et al.* (2016), who showed that monsoon onset over South Asia is coincident with the weakening of mid-level dry advection by northwesterlies over India; they argued that this mid-level dry advection suppresses moist convection and causes the onset of monsoon rains to occur earlier in southeastern India.

Near-surface moistening and mid-level drying by SMCs have thus been argued to alter the onset and subseasonal variability of monsoons in contrasting ways, and the same is true for their effect on seasonal mean monsoon precipitation. Haarsma *et al.* (2005) and Biasutti *et al.* (2009) found a negative correlation between summer-mean Sahel precipitation and low-level geopotential height (or surface pressure) over the Sahara, and argued that this indicated a stronger SMC was causing increased Sahel rainfall by drawing more moisture in from the ocean. However, Shekhar and Boos (2016) showed that the overturning circulation of the West African SMC is actually weaker when Sahel rainfall is enhanced, and that the negative correlation between Sahel precipitation and low-level geopotential occurred primarily because of a concurrent northward shift of the precipitation maximum and the SMC. The idea that Sahel precipitation is inhibited by a stronger SMC is supported by the results of Peyrillé and Lafore (2007), who found that the effect on precipitation of the mid-level warming and drying was stronger than that of the near-surface cooling and moistening when the two components of the vertical dipole were imposed separately in an idealized model. In separate work that did not even mention monsoons, Sobel and Bellon (2009) also found that advective drying in the middle troposphere can be highly effective at suppressing precipitation. They imposed drying tendencies at different levels of two single-column models, with these tendencies intended to represent horizontal moisture advection, and found that precipitation was more sensitive to middle-tropospheric drying than to lower-tropospheric drying. Their lower-tropospheric drying was imposed in the 825-600 hPa layer, and thus may be a better analogue for moisture advection in the upper branch of the SMC, but this nevertheless illustrates the potential for horizontal moisture advection at least a few kilometers above the surface to alter rainfall.

Although previous work has thus provided evidence for the suppression of monsoon precipitation by the horizontal advection of dry, mid-tropospheric air into the humid parts of West Africa, South Asia, and Australia, that previous work focused on a variety of time scales in a number of isolated regions. Regional intercomparisons and global analyses of SMCs have been conducted (e.g. Zhang *et al.* 2008; Trenberth *et al.* 2000), but these have examined SMC winds rather than the moisture advection produced by SMCs. It remains unclear whether the intensity and vertical structure of the drying tendencies produced by SMCs is similar across all monsoon regions, and whether advection by time-mean SMC winds dominates advection by transient eddies. One goal of this study is thus to document and compare the distributions of horizontal advective drying in four monsoon regions during local summer: West Africa, South Asia, southern Africa, and Australia. All of these regions have been shown to have prominent SMCs in the local summer mean (Nie *et al.* 2010). Here we ask, in particular, whether horizontal advective drying a few kilometers above the surface has comparable strength and vertical structure in all regions, and whether it is produced primarily by time mean winds or by transient eddies. Furthermore, if transient eddy advection of moisture is large, can it be represented as a simple down-gradient diffusion of moisture? It seems plausible, for example, that transient eddy advection of moisture might be stronger in West Africa than in other regions because of the prominence of African easterly waves, which are known to advect momentum meridionally (Reed *et al.* 1977; Straub *et al.* 2006, e.g.), and that it might not be possible to describe moisture transport by these waves in terms of a simple eddy diffusion. Resolution of these issues is important for constructing accurate conceptual and theoretical models of monsoons.

To be clear, we focus on horizontal rather than vertical advection in this paper because vertical motion cannot be viewed as a cause of precipitation. In contrast, horizontal flow in SMCs is controlled by boundary layer temperature gradients tied to surface conditions, and that flow produces horizontal advection that is more widely viewed as a control on precipitating convection. To illustrate this, we briefly introduce the vertically integrated moisture budget, following Seager and Henderson (2013),

$$P - E = -\frac{1}{g}\frac{\partial}{\partial t}\int_0^{p_s} q\,dp - \frac{1}{g}\int_0^{p_s} q\,(\nabla\cdot\mathbf{u})\,dp - \frac{1}{g}\int_0^{p_s} (\mathbf{u}\cdot\nabla q)\,dp - \frac{q_s}{g}\mathbf{u}_s\cdot\nabla p_s. \quad (1)$$

Here the difference between precipitation P and surface evapotranspiration E is balanced by the time rate of change of vertically integrated moisture, the convergence of horizontal wind $\mathbf{u}$ having specific humidity q, horizontal advection of humidity, and a boundary term that involves the surface values of horizontal wind, humidity, and pressure p (with g the gravitational acceleration). The second term on the right-hand side, which is often large, can alternately be expressed as vertical advection of moisture and thus depends on vertical motion. But in low latitudes,

vertical velocity cannot be viewed as a cause of precipitating convection; when the Coriolis parameter is small, weak horizontal temperature gradients allow vertical motion to be diagnosed from the diabatic heating in a selected column of the atmosphere (Sobel *et al.* 2001),

$$\omega \simeq \frac{Q_c}{S} \tag{2}$$

where Q_c is the convective heating and S is a static stability. The vertical integral of Q_c is equal to P on the left-hand side of (1), so under the weak temperature gradient approximation the vertical advective term in the moisture budget becomes a function of the precipitation itself and thus cannot be viewed as a control on precipitation. In contrast, horizontal flow in SMCs is regulated by the contrasts between deserts and adjacent vegetated or ocean regions and is not directly driven by precipitation. This is why numerical studies of precipitation in a single atmospheric column have imposed mid-tropospheric drying as an idealized proxy for horizontal moisture advection (e.g. Sobel and Bellon 2009), and why observational studies view horizontal moisture advection as a control on precipitation (e.g. Parker *et al.* 2016).

The next section of this paper describes the data used in this study. The time-mean structure and climatological seasonal cycle of SMCs over different continents are then presented in Section 3, followed by analyses of horizontal advective drying in Section 4. We summarize and discussion of implications in Section 5.

2. Data sources and analysis procedure

We used six-hourly data for 1979-2014 from ERA-Interim, the latest global atmospheric reanalysis from the European Centre for Medium-Range Weather Forecasts. We used data that was regridded to a resolution of approximately 0.7° × 0.7° in the horizontal with 37 pressure levels. For precipitation, we used estimates from the Tropical Rainfall Measuring Mission (TRMM) product 3B42 for 1998 to 2012, which provides 3-hourly precipitation rates at a horizontal resolution of 0.25° × 0.25°. Summer means were calculated over June-August for northern hemisphere monsoon regions and December-February for southern hemisphere regions, and all results presented here are climatologies averaged over all years of the relevant dataset.

Horizontal moisture advection by the total flow was directly computed using six-hourly ERA-Interim data, then these horizontal advective tendencies were averaged over the local summer periods of all of the 36 years in our ERA-Interim sample. The advection of moisture by transient eddies was calculated by subtracting the horizontal advective tendency produced by the time-mean flow (i.e. the climatological summer mean horizontal flow acting on the climatological mean specific humidity distribution) from the total horizontal advection.

3. Regional climatologies of shallow monsoon flow

We begin by briefly examining the climatological mean horizontal and vertical structure of SMCs in four monsoon regions during local summer. Although some properties of SMCs have been compared across different regions, these intercomparisons have focused more on the cross-equatorial flow rather than that in the off-equatorial monsoon precipitation maxima (e.g. Zhang *et al.* 2008). No intercomparison of the horizontal and vertical structures of these circulations and their relation with the distributions of humidity and monsoon precipitation has been published.

The summer-mean circulation in monsoon regions typically includes an anticyclone centered several kilometers above the surface, around 700 hPa (Fig. 1a, c, d). The lower-latitude part of each anticyclone constitutes the upper branch of the local SMC, in which equatorward flow is directed across strong horizontal gradients of relative humidity into the region of high precipitation (which is outlined in cyan in Fig. 1). These anticyclones are approximately in geostrophic balance: the scales of the Australian anticyclone, for example, yield a Rossby number less than 0.1.

Substantial regional differences exist in the horizontal structure and magnitude of flow in these SMCs. Equatorward flow in the upper branch of an SMC is strongest and most horizontally extensive in West Africa, where northeasterly winds with magnitude around 10 m s^{-1} stretch thousands of kilometers across the entire Sahel at 700 hPa (Fig. 1a). The horizontal structure of the 700 hPa anticyclone is highly asymmetric over West Africa, with southward flow on its eastern side much more zonally confined than northward flow on its western side. The anticyclones over southern Africa and Australia are more symmetric and have equatorward flow into the monsoon precipitation maximum that is weaker than that seen over West Africa (Fig. 1c, d; we show fields at 600 hPa for southern Africa because orography in that region seems to shift the SMC there to lower pressures, a phenomenon shown in more detail below). Flow in the higher-latitude halves of the Australian and southern African anticyclones has merged with the midlatitude westerlies, and it is primarily the eastern branch of these two anticyclones that is directed along a strong dry-to-moist horizontal gradient in relative humidity. In contrast, it is the southern part of the West African anticyclone that crosses isolines of relative humidity. The summer-mean humidity field over southern Africa seems to be highly distorted by the anticyclone, with a tongue of dry air wrapping around that anticyclone's center into the eastern side of the precipitating region.

The 700 hPa flow in South Asia is distinct from that in other regions, presumably because lower-tropospheric horizontal flow there is highly modified by orography. During boreal summer, strong low-level monsoon westerlies extend across the entire South Asian region between the equator and 15°N, and substantial precipitation falls over much of the Indian Ocean and continental India (Fig. 1b). The SMC is evident as northerly and northwesterly flow at 700 hPa across Pakistan, the northern Arabian Sea, and the northern two-thirds of India. This is outflow from the intense desert heat low centered over Pakistan and northwestern India (Bollasina *et al.* 2011), which has been shown to dry the lower and middle troposphere over continental India, particularly during early summer (Parker *et al.* 2016). The South Asian monsoon thus lacks a clear 700 hPa anticyclone positioned over a desert heat low. Nevertheless, time-mean southward and southeastward flow from the deserts of southwestern Asia clearly advects dry air into the monsoon region.

We now examine the vertical structure of shallow flow in each region by horizontally averaging meridional wind over land within boxes that demarcate the four monsoon regions. West African winds are averaged from 10° N to 20° N and 10° W to 25° E, which is similar to definitions of the Sahel used in previous studies (e.g. Janowiak 1988; Biasutti and Sobel 2009; Giannini *et al.* 2013). South Asian winds are averaged from 15° N to 30° N and 65° E to 90° E, a region that excludes the southern tip of India but includes nearly all of the rest of India, and parts of Nepal and Bangaldesh. Winds in southern Africa were averaged from 16° E to 35° E and from 14° S to 24°S; although southern Africa is sometimes not regarded as a major monsoon region, it is home to a seasonal precipitation maximum that exhibits many of the dynamical features of monsoons (McHugh 2004; Nie *et al.* 2010; Hurley and Boos 2013). Australian winds are averaged from 10° S to 25° S and 120° E to 145° E, an area that includes the "top end" rainfall that constitutes the Australian monsoon (Wheeler and McBride 2005; Colman *et al.* 2011; Wang and Ding 2008). Our exact choice of boundaries in each region was guided by the desire to include regions with equatorward flow in the lower mid-troposphere, ensuring that our regional averages characterize the

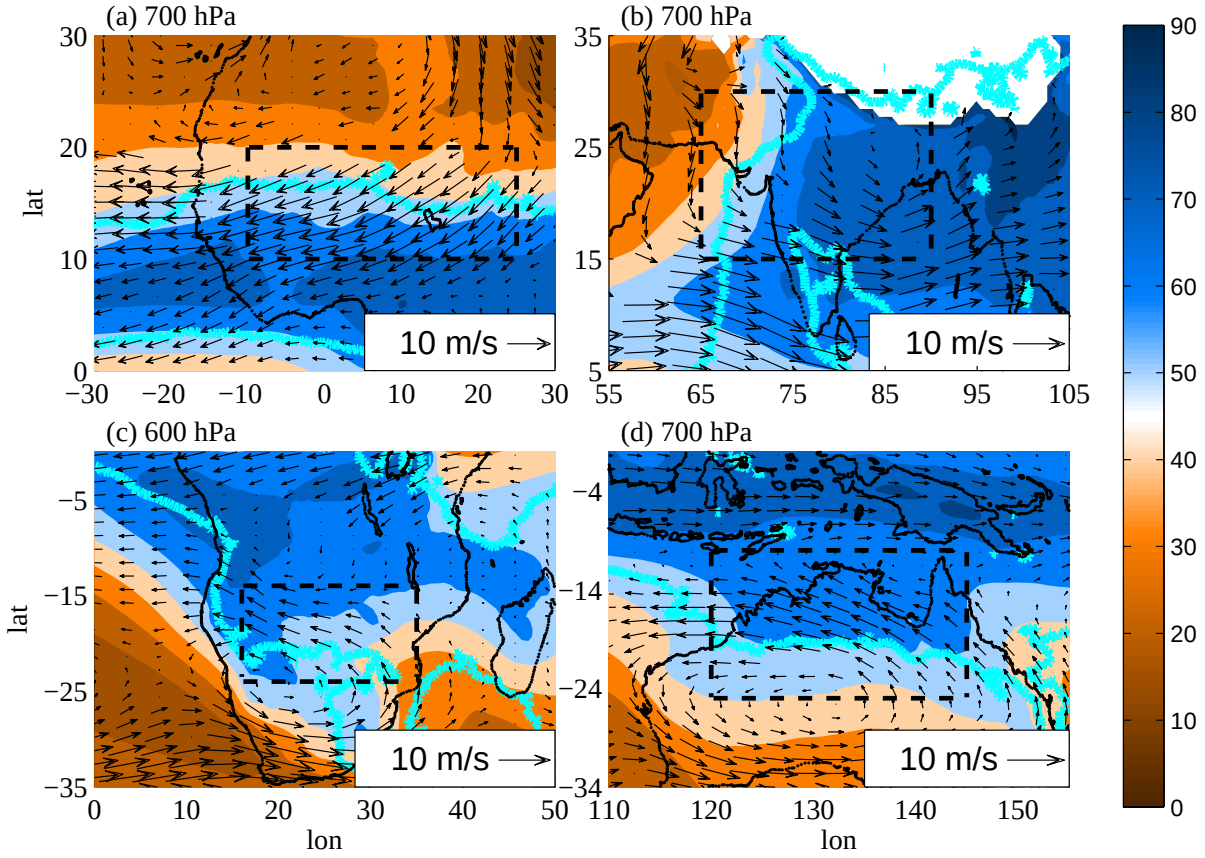

Figure 1. Relative humidity (RH, shading) in %, and horizontal velocity (vectors), in m s^{-1}, averaged June-August for **a)** West Africa and **b)** South Asia, and averaged December-January for **c)** southern Africa and **d)** Australia. The horizontal velocity and RH are shown at 600 hPa for southern Africa and at 700 hPa for other regions. The cyan line surrounds regions where the precipitation is larger than 2 mm day^{-1}, 4 mm day^{-1}, 3 mm day^{-1}, and 4 mm day^{-1} for West Africa, South Asia, southern Africa and Australia, respectively. The dashed rectangular boxes mark regions over which horizontal means are shown in later figures.

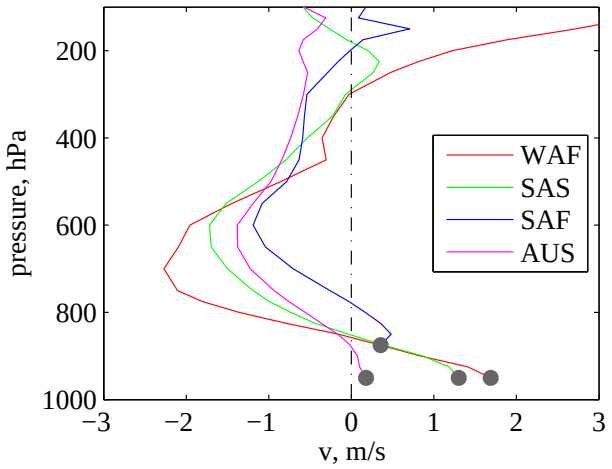

Figure 2. Vertical profiles of meridional velocity during local summer over West Africa (red), South Asia (green), southern Africa (blue) and Australia (magenta), averaged over land regions within the boxes shown in Fig. 1. Negative values indicate equatorward flow and positive indicate poleward flow. Data below the time- and horizontal-mean surface pressure level (which is marked by the gray circles) are not presented.

local SMC. Averages were taken only over land within each of these boxes in order to make our results relevant to continental precipitation, but including ocean regions yielded qualitatively similar results.

Comparison of the regionally averaged meridional wind shows that the vertical structure of SMCs is highly similar across all four monsoon areas (Fig. 2; the sign of meridional wind has been chosen so that poleward flow is positive). Low-level poleward flow in all regions is confined within 150 hPa of Earth's surface, and the upper branch of the SMC is evident as equatorward flow that peaks between 600 and 700 hPa. The transition from poleward to equatorward flow occurs at about 850 hPa in all regions except southern Africa. Our southern Africa region has a mean surface pressure around 900 hPa, and this reduced surface pressure is associated with a lifting of the entire vertical structure of the SMC. The upper branch of the SMC is strongest in West Africa and weakest over southern Africa.

Above the SMC, the vertical structure of the meridional wind has large regional differences. Upper-tropospheric flow over West Africa is poleward because the Sahel lies north of the African monsoon precipitation maximum; Sahelian upper-level flow is thus characteristic of the summer cell of the solsticial Hadley circulation. In contrast, our Australian and South Asian averages are dominated by the regional upper-tropospheric anticyclones. Northern Australia lies slightly closer to the eastern branch of that upper-tropospheric anticyclone (not shown) and thus exhibits equatorward flow at 200 hPa, while India lies closer to the western part of the upper-tropospheric anticyclone and so has poleward 200 hPa flow. The low-level mass-weighted, vertically integrated poleward mass flux appears to be substantially less than the equatorward mass flux in the upper branch of the SMC, but this is partly an artifact of plotting only values at pressures lower than the time-mean, regional-mean surface pressure (although the meridional flow need not vertically integrate to zero since it is averaged over a limited range of longitudes). For instance, in South Asia near-surface poleward flow is directed through the

eastern and western ends of the Indo-Gangetic plain, near sea level in a region where the mean surface elevation is substantially higher (e.g. Boos and Hurley 2013, their Fig. 3). Since the main focus of this paper is the advective drying in the upper branch of the SMC, we do not attempt to accurately diagnose the time-mean near-surface poleward mass flux in each region.

In summary, all four monsoon regions contain time-mean shallow circulations, with West Africa's being the strongest and southern Africa's the weakest. The upper part of these shallow circulations consists of an anticyclone centered near 700 hPa, except in South Asia where the horizontal structure of the flow is highly distorted by orography. The vertical structure of the regionally averaged meridional mass flux is highly similar across all regions, with the equatorward mass flux in the upper branch of the SMCs peaking at 600-700 hPa and spanning a layer of the middle troposphere that is roughly 500 hPa thick. The structure of the wind and humidity fields at 700 hPa suggests that these time-mean shallow circulations advect mid-tropospheric dry air into the precipitating monsoon regions (e.g. Fig. 1) — this moisture advection is examined in more detail in the next section.

4. Drying tendency of shallow flow

To begin our study of the mid-level drying produced by SMCs, we first examine the vertical distribution of horizontal moisture advection averaged over each of the continental regions described above. As expected, these vertical profiles of total horizontal moisture advection show a general pattern of near-surface moistening and mid-level drying (Fig. 3). The peak advective moistening occurs near the surface while the peak drying lies between 750-800 hPa. The peak drying occurs at lower altitudes than the peak equatorward wind (compare with Fig. 2) because the scale height of water vapor, roughly 2 km, is smaller than the depth of the SMC. The peak mid-level drying is of similar magnitude across all regions, peaking between 0.5 and 1 g kg^{-1}day^{-1}. The vertical profile for West Africa agrees with that computed by Peyrillé and Lafore (2007).

The relative contribution of time-mean flow and transient eddies to the total moisture advection varies greatly between regions. Advection of time-mean humidity by time-mean winds accounts for most of the total horizontal advection in both of our northern hemisphere monsoon regions, while advection by transient eddies is more important in the southern hemisphere regions (compare dashed and solid lines in Fig. 3). Transient eddy advection is particularly strong over northern continental Australia, where it accounts for at least 80% of the peak total horizontal advection. This disproves the idea that advective drying by transient eddies will be strongest over West Africa because of the prominence of African Easterly Waves. Although oceanic regions were excluded from the horizontal averages for South Asia and Australia, including those oceanic regions does not qualitatively change the vertical profiles of total or eddy drying tendencies (not shown).

Additional insight can be gained by examining the horizontal distribution of horizontal moisture advection, and we do so on the pressure level at which the maximum drying tendency occurs (800 hPa for South Asia, 775 hPa for Australia, and 750 hPa for West Africa and southern Africa). The advective drying is has strong horizontal inhomogeneity in South Asia, where the west coast of India shows particularly intense drying by horizontal advection. This is one region where the idea that horizontal advective drying can be viewed as a forcing for precipitation breaks down, because much precipitation in this region is forced by large-scale ascent over the orography of the Western Ghats; horizontal and vertical advection of moisture will strongly cancel each other when large-scale flow ascends along those mountain slopes. Over the rest of non-peninsular India, though, the horizontal advective drying is more uniform in the horizontal and can be attributed to the dry, northwesterly flow discussed by Parker *et al.* (2016). South Asia is also the only region that exhibits strong drying by horizontal advection over large parts of the ocean, particularly over the eastern Arabian Sea. That unique feature exists because strong westerly outflow from the Somali jet is superimposed on a strong zonal humidity gradient (Fig. 2b). In all other regions the horizontal advection around 800 hPa produces drying over continents and weaker moistening over ocean, often with a sharp boundary between the two at the coast.

Since transient eddies produce a large fraction of the total horizontal moisture advection in some regions, we wish to better understand the distribution and general nature of this eddy advection. As expected from the regionally averaged vertical profiles of advection discussed above, the horizontal distribution of advective drying by transient eddies is similar to that of the total horizontal advection in southern Africa and in Australia (compare bottom panels of Figs. 5 and 4, noting the change in color scale). This similarity is particularly strong in Australia; in southern Africa the eddy drying is strongest over the western part of our continental box while the total advective drying is strongest in the eastern part of that box. Eddy drying is weak over India and West Africa, although eddy moistening is strong over the southwestern coast of India.

One common way to represent the horizontal advection produced by transient eddies is via an "eddy diffusion" that acts on the time-mean quantity being advected. In an idealized model, Sobel and Neelin (2006) showed that the intensity and meridional width of the intertropical convergence zone (ITCZ) could be controlled by changing the horizontal eddy diffusion of moisture. In this spirit, we calculated the two-dimensional Laplacian of specific humidity on the same pressure levels used for plotting the horizontal distributions of transient eddy advection, and multiplied this by a constant diffusivity of 5×10^5 m^2 s^{-1}. This diffusivity was chosen subjectively to roughly match the observed magnitude of the transient eddy advective drying, but it lies in the range of values used in idealized models for tropical dynamics (e.g. Neelin and Zeng 2000; Sobel and Neelin 2006). Since the second derivatives in the Laplacian produce high variance at fairly short spatial scales, we introduced a weak smoothing by applying a 1-2-1 filter one time each in latitude and longitude. Additional smoothing could be obtained by successive application of this filter.

Our parameterized eddy diffusion matches the transient eddy advection most closely in the southern hemisphere (Fig. 6; an isoline of eddy diffusion is superimposed on the transient eddy advection in Fig. 5 to ease comparison). Although most features in the spatial distribution of the eddy diffusion are too sharp, the diffusive drying otherwise matches the eddy advective drying well over the coastal regions of Australia, southern Africa, Madagascar, and Indonesia/Papua New Guinea. The agreement is poorer over South Asia and West Africa. One particularly notable disagreement is in the Atlantic ITCZ, where the diffusive estimate predicts drying of about 0.5 g kg^{-1}day^{-1} while the transient eddy advection is close to zero and the total horizontal moisture advection produces moistening in the eastern part of that region (compare first panels of Figs. 4-6). Weak moisture advection in the eastern Atlantic ITCZ by the time-mean horizontal wind is expected because the time-mean wind is directed parallel to that ITCZ; the mid-tropospheric Saharan anticyclone does not produce southward flow as far south as that ITCZ region, and the eddy moisture advection produced by African Easterly Waves seems to be weak there.

To the degree that transient eddy advection can be represented by a diffusive approximation over continental Australia and

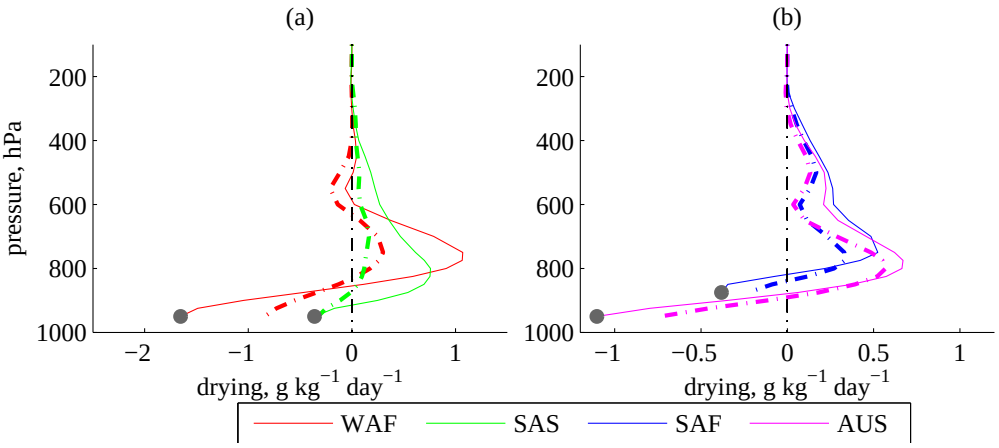

Figure 3. Vertical profiles of horizontal moisture advection, $\overline{\mathbf{u}\cdot\nabla q}$, averaged during local summers and over land in the boxes indicated in Fig. 1. Units are g kg^{-1} day^{-1} and colors correspond to the same regions as in Fig.2. The sign is chosen so that a positive number denotes a drying tendency. Solid lines show the tendency produced by the total flow and dashed lines show the tendency produced by transient eddies. Gray circles mark the time- and horizontal-mean surface pressure.

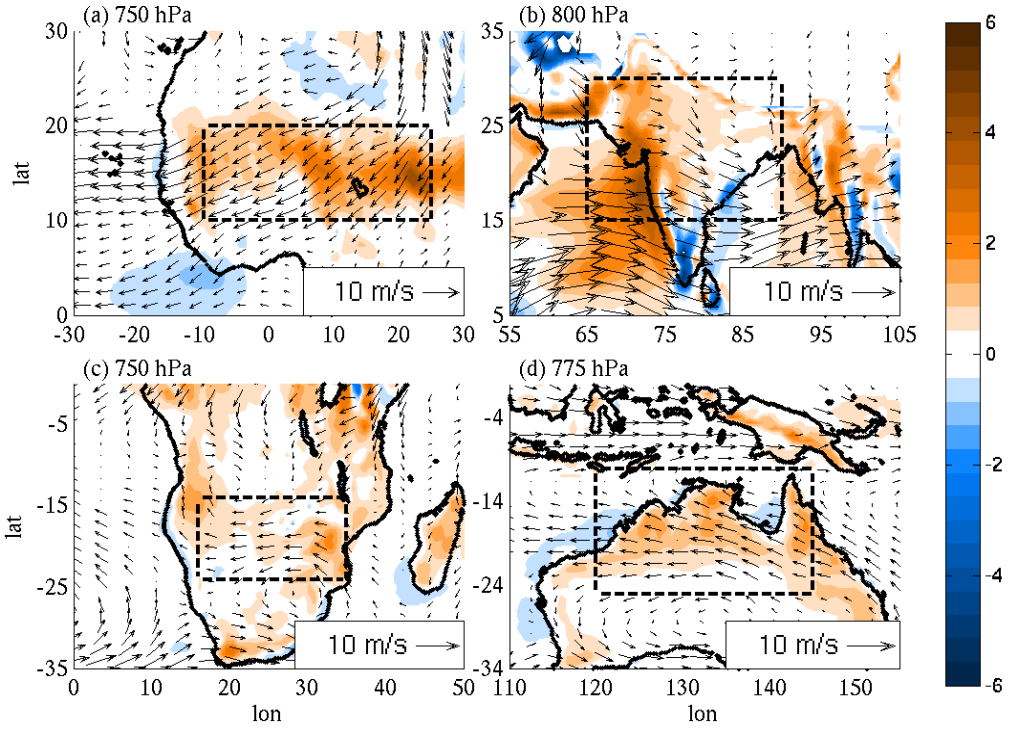

Figure 4. Drying tendency ($\overline{\mathbf{u}\cdot\nabla q}$, shading, in g kg^{-1} day^{-1}) and horizontal wind (vectors, in m s^{-1}) averaged during local summer. In each region these quantities are plotted at the level at which the regionally averaged drying tendency (shown in Fig. 3) is maximum: 750 hPa, 800 hPa, 750 hPa and 775 hPa for West Africa, South Asia, southern Africa and Australia, respectively. The contour interval for the shading is 0.4 g kg^{-1} day^{-1}.

southern Africa, eddy drying should not be thought of as being large only in regions where there is a local humidity maximum. That is, eddy diffusion is large where the curvature of the humidity field is large, and large curvature often occurs in regions far from humidity maxima (we do not show the time-mean specific humidity field because it looks very much like the relative humidity field shown in Fig. 1). For example, diffusive drying is strong over coastal Australia, but one would have a difficult time identifying a region of strong curvature there by eye. In contrast, the humidity field has a local maximum over Papua New Guinea (Fig. 1d), which produces strong diffusive drying there (Fig. 6d). Although these distributions of diffusive drying are a straightforward consequence of the approximation of the diffusive flux as being proportional to the humidity gradient, they provide a useful reminder that transient eddy drying need not occur in only the most humid regions.

What consequence might these distributions of advective drying have for monsoon precipitation? In an idealized model of a single column of the atmosphere, Sobel and Bellon (2009) found that a drying tendency of 1 g kg^{-1}day^{-1} in the 600-825 hPa layer produced a rainfall reduction of about 10 mm day^{-1}. Thus, the advective drying shown in Fig. 4 would seem to be sufficiently large to produce strong reduction in rainfall. The effect of this mid-tropospheric drying would be opposed by that of the near-surface moistening, and horizontal temperature advection will also influence precipitation. As mentioned in the Introduction, Peyrillé and Lafore (2007) found that the negative effect of mid-level warming and drying on an idealized simulation of Sahel rainfall was stronger than the positive effect of near-surface cooling and moistening. But they showed results only for 20 simulated days in one zonally symmetric model, so further investigation seems warranted.

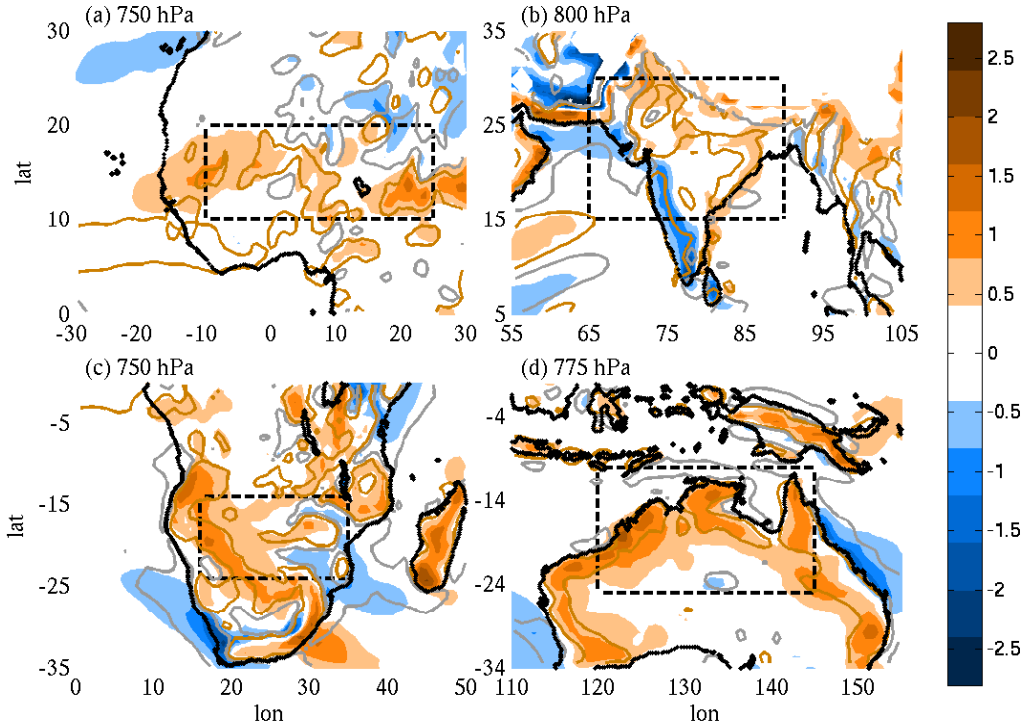

Figure 5. Drying tendency by transient eddies ($\overline{\mathbf{u}' \cdot \nabla q'}$, shading, in g kg^{-1} day^{-1}), averaged during local summer at the same levels as in Fig. 4. The contour interval is 0.4 g kg^{-1} day^{-1}, as in Fig. 4, but note the smaller range used for the color scale. Solid contours outline regions where our eddy moisture diffusion (see text for details) has a magnitude larger than 0.4 g kg^{-1} day^{-1}, with the orange contour signifying diffusive drying and the gray diffusive moistening.

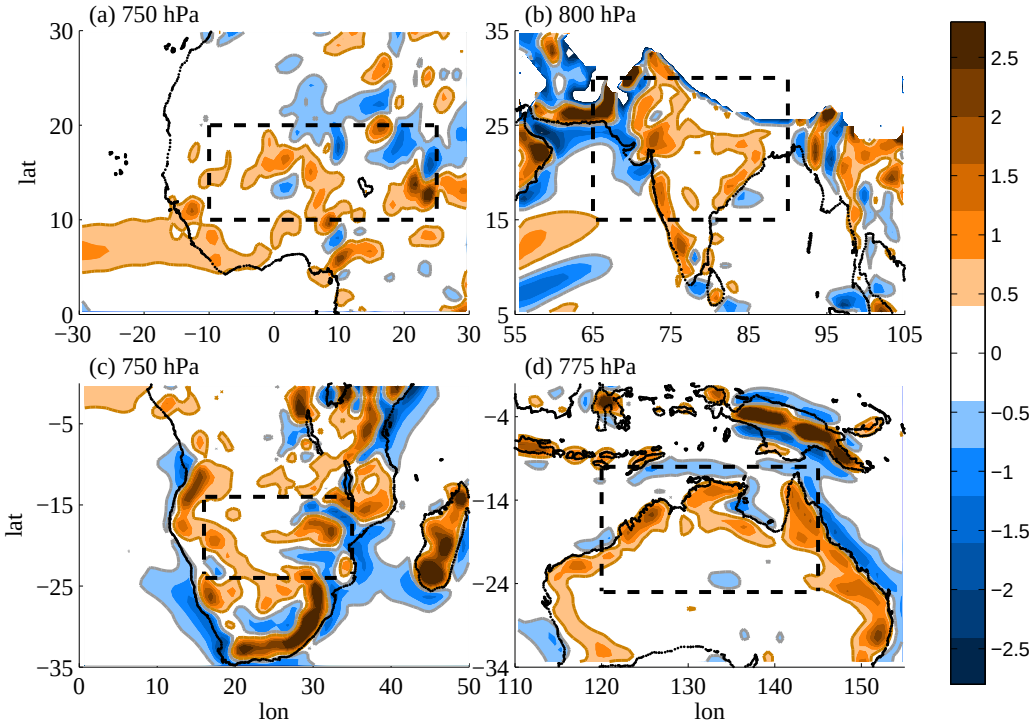

Figure 6. The field of moisture diffusion in laplacian form with a diffusivity of 5x10^5 m^2 s^{-1}. For shadings, orange stands for drying and blue for moistening, plotted with an interval of 0.4 g kg^{-1} day^{-1}. For contours, orange and grey are the 0.4 g kg^{-1} day^{-1} and -0.4 g kg^{-1} day^{-1}, respectively, with a 1-2-1filter applied for one time.

The seasonal cycle of precipitation and mid-tropospheric drying tendency in West Africa and South Asia is consistent with the hypothesis that advective drying inhibits precipitation. In West Africa the advective drying at 700 hPa peaks in June (near calendar day 160), then decreases as summer progresses and the precipitation rate increases (Fig. 7). Advective drying at 700 hPa over the Sahel is about half as strong in August-September as it is in June. Zhang *et al.* (2008) suggested that the West African SMC might inhibit the northward migration of precipitation over the Sahel during early summer by advecting "dry, warm, and

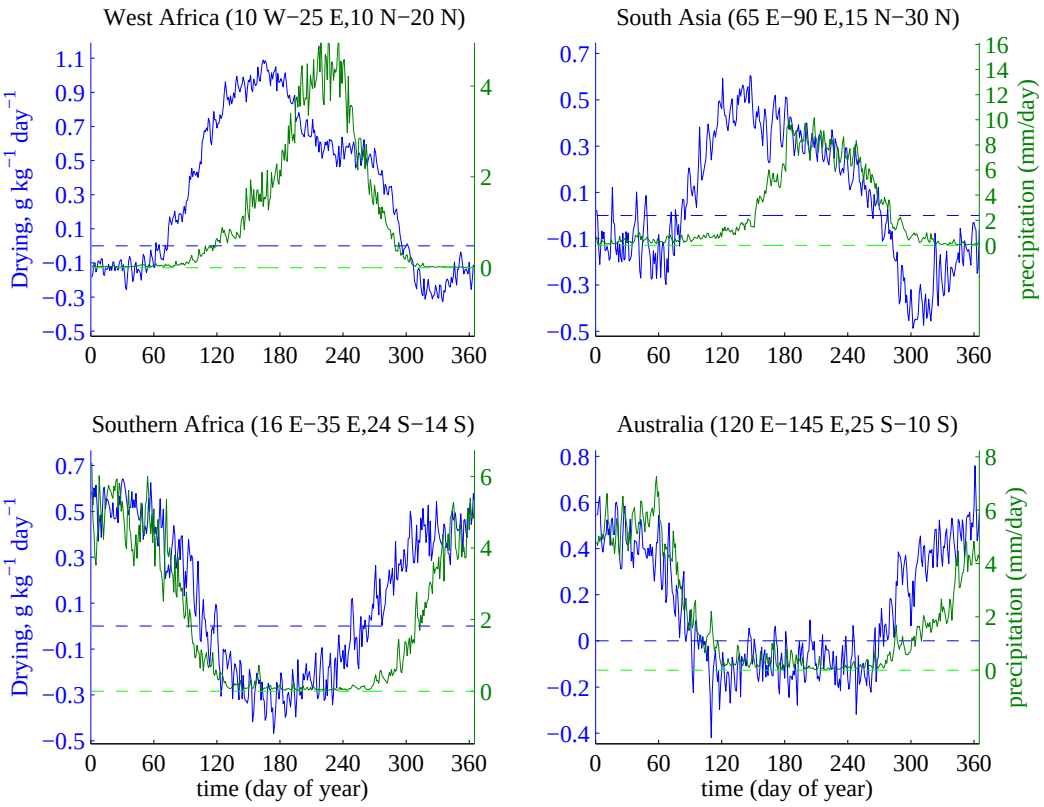

Figure 7. Daily climatologies of the advective drying tendency in g kg^{-1} day^{-1} at 700 hPa (blue solid) and of precipitation in mm/day (green solid), horizontally averaged over land in the boxes indicated in Fig. 1. Horizontal dashed lines mark zero for advective drying (blue) and precipitation (green).

perhaps dusty, air from the heat low into the monsoon rainband" (see also Parker *et al.* 2005), but to our knowledge no one has actually documented the seasonal cycle of advective drying in that region. Advective drying in South Asia is also stronger prior to the onset of summer rainfall. In contrast, there is no clearly discernable decrease in advective drying that accompanies the onset of summer rainfall in Australia and southern Africa. In those regions advective drying increases in spring (from day 250-300), and does not decrease when summer precipitation starts around day 320. The fact that the advective drying decreases most strongly during monsoon onset in West Africa may be due to the comparatively high amplitude of the advective drying in West Africa. The advective drying has a similarly strong magnitude over western India (Fig. 4, and its gradual summer decrease in our South Asian box would be consistent with the finding of (Parker *et al.* 2016) that precipitation spreads to the northwest over India while the advective drying contracts to the northwest.

5. Summary and discussion

Here we documented the climatological summer mean structure of SMCs in the monsoon regions of West Africa, South Asia, southern Africa and Australia, then compared the horizontal advective drying tendency produced by time-mean flow in those SMCs with that produced by transient eddies. Regionally averaged equatorward flow in the lower mid-troposphere is strongest over West Africa and weakest in southern Africa, as is the advective drying tendency. Equatorward flow in the SMC peaks near 600-700 hPa in all regions, while the peak drying tendency peaks between 750-800 hPa. The time-mean flow produces most of the summer mean horizontal moisture advection in West Africa and South Asia, while drying by transient eddies dominates in Australia and southern Africa. Although transient eddies are especially well-known in West Africa (i.e. African Easterly Waves), the advective drying produced by transient eddies is stronger over Australia and southern Africa, where this eddy drying can be well-represented as a simple harmonic diffusion with a diffusivity around 5×10^5 m^2 s^{-1}. This result is important for our understanding of monsoons because it means that horizontal moisture advection can be accounted for by knowing the time-mean flow and the time-mean humidity distribution. Existing theoretical models of monsoons (e.g. Emanuel 1995; Neelin and Zeng 2000; Boos and Emanuel 2008) contain only a barotropic and first-baroclinic mode, and detailed knowledge of the vertical structure of SMCs and their influence on the moisture field is needed to construct models with additional vertical degrees-of-freedom.

We hope that future work will explore how the strength and vertical structure of SMCs are related to gradients in surface pressure, boundary-layer temperature, and surface sensible and latent heat fluxes. Perhaps even more important is the detailed examination of the sensitivity of monsoon precipitation to near-surface cooling and moistening combined with elevated warming and drying. Recent work has compiled linear sensitivities of moist convection to isolated temperature and humidity tendencies using cloud-system resolving models integrated with oceanic lower boundary conditions (Kuang 2010; Tulich and Mapes 2010); application of those linear frameworks to the monsoon systems examined here may help in understanding the seasonal evolution and interannual variability of monsoon rainfall. More fundamentally, we would like to know whether the influence of horizontal moisture advection alters continental monsoon precipitation in the same way that it does oceanic precipitation, and whether the sensitivity is fundamentally altered by dynamical feedbacks with the large-scale monsoon flow.

References

Austin JM, Fleisher A. 1948. A thermodynamic analysis of cumulus convection. *Journal of Meteorology* **5**(5): 240–243.

Biasutti M, Sobel AH. 2009. Delayed seasonal cycle and African monsoon in a warmer climate. *arXiv preprint arXiv:0907.2735* .

Biasutti M, Sobel AH, Camargo SJ. 2009. The role of the Sahara low in summertime Sahel rainfall variability and change in the CMIP3 models. *Journal of Climate* **22**(21): 5755–5771.

Bollasina MA, Ming Y, Ramaswamy V. 2011. Anthropogenic aerosols and the weakening of the South Asian summer monsoon. *Science* **334**(6055): 502–505.

Boos WR. 2015. A review of recent progress on Tibet's role in the South Asian monsoon. *CLIVAR Exchanges* **19**(66): 23–27.

Boos WR, Emanuel KA. 2008. Wind-evaporation feedback and abrupt seasonal transitions of weak, axisymmetric Hadley circulations. *Journal of the Atmospheric Sciences* **65**(7): 2194–2214.

Boos WR, Hurley JV. 2013. Thermodynamic bias in the multimodel mean boreal summer monsoon*. *Journal of Climate* **26**(7): 2279–2287.

Boos WR, Kuang Z. 2010. Dominant control of the South Asian monsoon by orographic insulation versus plateau heating. *Nature* **463**(7278): 218–222.

Chakraborty A, Nanjundiah R, Srinivasan J. 2006. Theoretical aspects of the onset of Indian summer monsoon from perturbed orography simulations in a GCM. *Annales Geophysicae* **24**(8): 2075–2089.

Chou C, Neelin J, Su H. 2001. Ocean-atmosphere-land feedbacks in an idealized monsoon. *Quarterly Journal of the Royal Meteorological Society* **127**(576): 1869–1891.

Colman R, Moise A, Hanson L. 2011. Tropical Australian climate and the Australian monsoon as simulated by 23 CMIP3 models. *Journal of Geophysical Research: Atmospheres* **116**(D10).

Derbyshire S, Beau I, Bechtold P, Grandpeix JY, Piriou JM, Redelsperger JL, Soares P. 2004. Sensitivity of moist convection to environmental humidity. *Quarterly Journal of the Royal Meteorological Society* **130**(604): 3055–3079.

Emanuel KA. 1995. The behavior of a simple hurricane model using a convective scheme based on subcloud-layer entropy equilibrium. *Journal of the Atmospheric Sciences* **52**(22): 3960–3968.

Giannini A, Salack S, Lodoun T, Ali A, Gaye A, Ndiaye O. 2013. A unifying view of climate change in the Sahel linking intra-seasonal, interannual and longer time scales. *Environmental Research Letters* **8**(2): 024 010.

Gu G, Adler RF. 2004. Seasonal evolution and variability associated with the West African monsoon system. *Journal of Climate* **17**(17): 3364–3377.

Haarsma RJ, Selten FM, Weber SL, Kliphuis M. 2005. Sahel rainfall variability and response to greenhouse warming. *Geophysical Research Letters* **32**(17).

Holloway CE, Neelin JD. 2009. Moisture vertical structure, column water vapor, and tropical deep convection. *Journal of the Atmospheric Sciences* **66**(6): 1665–1683.

Hurley JV, Boos WR. 2013. Interannual variability of monsoon precipitation and local subcloud equivalent potential temperature. *Journal of Climate* **26**(23): 9507–9527.

Janowiak JE. 1988. An investigation of interannual rainfall variability in Africa. *Journal of Climate* **1**(3): 240–255.

Kawamura R, Fukuta Y, Ueda H, Matsuura T, Iizuka S. 2002. A mechanism of the onset of the Australian summer monsoon. *Journal of Geophysical Research: Atmospheres (1984–2012)* **107**(D14): ACL–5.

Kuang Z. 2010. Linear response functions of a cumulus ensemble to temperature and moisture perturbations and implications for the dynamics of convectively coupled waves. *Journal of the Atmospheric Sciences* **67**(4): 941–962.

McHugh MJ. 2004. Near-surface zonal flow and East African precipitation receipt during austral summer. *Journal of Climate* **17**(20): 4070–4079.

Neelin JD, Zeng N. 2000. A quasi-equilibrium tropical circulation model—Formulation. *Journal of the Atmospheric Sciences* **57**(9).

Nie J, Boos WR, Kuang Z. 2010. Observational evaluation of a convective quasi-equilibrium view of monsoons. *Journal of Climate* **23**(16): 4416–4428.

Nolan DS, Zhang C, Chen Sh. 2007. Dynamics of the shallow meridional circulation around intertropical convergence zones. *Journal of the Atmospheric Sciences* **64**(7): 2262–2285.

Parker D, Burton R, Diongue-Niang A, Ellis R, Felton M, Taylor C, Thorncroft C, Bessemoulin P, Tompkins A. 2005. The diurnal cycle of the West African monsoon circulation. *Quarterly Journal of the Royal Meteorological Society* **131**(611): 2839–2860.

Parker DJ, Willetts P, Birch C, Turner AG, Marsham JH, Taylor CM, Kolusu S, Martin GM. 2016. The interaction of moist convection and mid-level dry air in the advance of the onset of the Indian monsoon. *Quarterly Journal of the Royal Meteorological Society* .

Peixoto JP, Oort AH. 1992. *Physics of Climate*. New York, NY (United States); American Institute of Physics.

Peyrillé P, Lafore JP. 2007. An idealized two-dimensional framework to study the West African monsoon. Part II: Large-scale advection and the diurnal cycle. *Journal of the Atmospheric Sciences* **64**(8): 2783–2803.

Privé NC, Plumb RA. 2007. Monsoon dynamics with interactive forcing. Part I: Axisymmetric studies. *Journal of the Atmospheric Sciences* **64**(5): 1417–1430.

Reed RJ, Norquist DC, Recker EE. 1977. The structure and properties of African wave disturbances as observed during Phase III of GATE. *Monthly Weather Review* **105**(3): 317–333.

Seager R, Henderson N. 2013. Diagnostic computation of moisture budgets in the ERA-Interim reanalysis with reference to analysis of CMIP-Archived atmospheric model data*. *Journal of Climate* **26**(20): 7876–7901.

Shekhar R, Boos WR. 2016. Weakening and shifting of the Saharan heat low circulation during wet years of the West African monsoon. *arXiv preprint arXiv:1609.08515* .

Sherwood SC. 1999. Convective precursors and predictability in the tropical western Pacific. *Monthly Weather Review* **127**(12): 2977–2991.

Sobel AH, Bellon G. 2009. The effect of imposed drying on parameterized deep convection. *Journal of the Atmospheric Sciences* **66**(7): 2085–2096.

Sobel AH, Neelin JD. 2006. The boundary layer contribution to intertropical convergence zones in the quasi-equilibrium tropical circulation model framework. *Theoretical and Computational Fluid Dynamics* **20**(5-6): 323–350.

Sobel AH, Nilsson J, Polvani LM. 2001. The weak temperature gradient approximation and balanced tropical moisture waves*. *Journal of the Atmospheric Sciences* **58**(23): 3650–3665.

Straub KH, Kiladis GN, Ciesielski PE. 2006. The role of equatorial waves in the onset of the South China Sea summer monsoon and the demise of El Niño during 1998. *Dynamics of Atmospheres and Oceans* **42**(1): 216–238.

Sultan B, Janicot S, *et al.* 2000. Abrupt shift of the ITCZ over West Africa and intra-seasonal variability. *Geophys. Res. Lett* **27**(20): 3353–3356.

Thorncroft CD, Nguyen H, Zhang C, Peyrille P. 2011. Annual cycle of the West African monsoon: regional circulations and associated water vapour transport. *Quarterly Journal of the Royal Meteorological Society* **137**(654): 129–147.

Tompkins AM. 2001. Organization of tropical convection in low vertical wind shears: The role of water vapor. *Journal of the Atmospheric Sciences* **58**(6): 529–545.

Trenberth KE, Stepaniak DP, Caron JM. 2000. The global monsoon as seen through the divergent atmospheric circulation. *Journal of Climate* **13**(22): 3969–3993.

Tulich SN, Mapes BE. 2010. Transient environmental sensitivities of explicitly simulated tropical convection. *Journal of the Atmospheric Sciences* **67**(4): 923–940.

Wang B, Ding Q. 2008. Global monsoon: Dominant mode of annual variation in the tropics. *Dynamics of Atmospheres and Oceans* **44**(3): 165–183.

Wheeler M, McBride J. 2005. Australian-Indonesian monsoon. In: *Intraseasonal variability in the atmosphere-ocean climate system*, Springer, pp. 125–173.

Xie S, Hume T, Jakob C, Klein SA, McCoy RB, Zhang M. 2010. Observed large-scale structures and diabatic heating and drying profiles during TWP-ICE. *Journal of Climate* **23**(1): 57–79.

Yoneyama K, Parsons DB. 1999. A proposed mechanism for the intrusion of dry air into the tropical western Pacific region. *Journal of the Atmospheric Sciences* **56**(11): 1524–1546.

Zhang C, McGauley M, Bond NA. 2004. Shallow meridional circulation in the tropical eastern Pacific*. *Journal of Climate* **17**(1): 133–139.

Zhang C, Nolan DS, Thorncroft CD, Nguyen H. 2008. Shallow meridional circulations in the tropical atmosphere. *Journal of Climate* **21**(14): 3453–3470.